



A comprehensive study of glucose transfer in the human small intestine using an *in vitro* intestinal digestion system (i-IDS) based on a dialysis membrane process



Minghai Gim-Krumm^a, Pablo Donoso^a, Rommy N. Zuñiga^{b,c}, Humberto Estay^d, Elizabeth Troncoso^{a,*}

^a Department of Chemistry, Universidad Tecnológica Metropolitana, Las Palmeras, 3360 Ñuñoa, Santiago, Chile

^b Department of Biotechnology, Universidad Tecnológica Metropolitana, Las Palmeras, 3360 Ñuñoa, Santiago, Chile

^c Programa Institucional de Fomento a la Investigación, Desarrollo e Innovación, Universidad Tecnológica Metropolitana, Ignacio Valdivieso, 2409 San Joaquín, Santiago, Chile

^d Advanced Mining Technology Center (AMTC), University of Chile, Chile

ARTICLE INFO

Keywords:

Glucose absorption
Human small intestine
In vitro digestion
Hollow fiber membranes modules
Modeling

ABSTRACT

Human digestion is a complex process that involves several phenomena: chemical and enzymatic reactions, absorption, hydrodynamic processes, and mass transfer. The most accurate way to determine the bioavailability of different nutrients is through human studies. However, there are ethical, economic, and technical reasons that restrict their application. Aiming at contributing with a new experimental prototype and phenomenological model to study nutrient absorption in the human small intestine, an *in vitro* intestinal digestion system (i-IDS), based on a hollow fiber dialysis membrane process, was constructed and tested under different operational conditions of feed flow/dialysate flow ratio. This dialysis membrane process here presented, allowed to simulate and extrapolate results of the process of glucose transfer in the human small intestine, where the glucose mass transfer reached around 90% at times ranging between 25 and 40 min. The mathematical model was validated with respect to the experimental results, obtaining a good agreement (root mean square error, %RMS, between 3% and 19%) among them. Overall permeabilities for the experimental conditions ranged between 3.85×10^{-6} and 4.86×10^{-6} m³/s. The experimental results of glucose absorption were extrapolated to those found in the human small intestine using a phenomenological model, where a good agreement among results of glucose absorption was found in human studies. This first experimental and phenomenological approach allows to acquire a better knowledge of the complex mass transfer processes found in human small intestine for nutrient absorption.

1. Introduction

1.1. *In vitro* systems to simulate human digestion

Human digestion is a complex process wherein several chemical, enzymatic, and mechanical phenomena occur. The gastrointestinal tract (GIT) can be viewed as a versatile multi-compartment reactor that operates on a variable solid/liquid feed but delivers more or less standardized products [1]. Human studies are the most accurate way of determining the bioavailability of different foods, but there are ethical, economic and technical reasons that restrict their application [2–4]. Despite these limitations, several *in vitro* digestion systems have been developed to predict the *in vivo* behavior of foods during digestion and

absorption.

The construction of *in vitro* digestion systems is challenging because of the complex biochemical and mechanical phenomena present in the GIT. The use of realistic digestion systems is a key feature to generate *in vitro* results comparable to *in vivo* data [5]. To date, most of the studies have focused on fabricating gastric models [2,6–10], but few models have been developed to simulate the small intestine or other parts of the GIT [11]. However, intestinal absorption is critical in determining bioavailability, because what is exclusively absorbed can be then used by the human body. Simple artificial or biological membrane systems or assays based on biological cell monolayers (e.g. Caco-2 cells) [12,13] have been used to simulate the *in vitro* absorption. According to Marze [5], a limitation of most *in vitro* intestinal models is the difficulty to

* Corresponding author.

E-mail address: elizabeth.troncoso@utem.cl (E. Troncoso).

<https://doi.org/10.1016/j.memsci.2018.07.080>

Received 26 May 2018; Received in revised form 3 July 2018; Accepted 27 July 2018

Available online 29 July 2018

0376-7388/ © 2018 Elsevier B.V. All rights reserved.

Nomenclature	
1	Subscript of the equipment input conditions.
2	Subscript of the equipment output conditions
φ	Packing fraction of the module ($\varphi = n[d_{out}/D_s]^2$)
ΔC_g	Concentration difference between the bulk of the feed and dialysate phases (kg/m ³)
ΔP	Transmembrane pressure (Pa)
ε	Porosity of the fibers
ρ_{water}	Water density (kg/m ³)
τ	Tortuosity of the fibers
μ_{water}	Water viscosity (kg/ms)
A_T	Total area of mass transfer (m ²)
C_g^0	Initial glucose concentration (kg/m ³)
C_g^F	Concentration of glucose in the bulk of the feed solution (kg/m ³)
C_g^D	Concentration of glucose in the bulk of the dialysate solution (kg/m ³)
CL	Characteristic length (e.g. internal diameter for the membrane lumen side and equivalent diameter for the shell side). The characteristic length of the shell side is defined by the equivalent or hydraulic diameter as d_h ($4 \times [\text{flow surface area}]/[\text{wetted perimeter}]$)
$D_{glucose-water}$	Diffusion coefficient of glucose in water (m ² /s)
D_s	Shell inside diameter (m)
d_{in}	Inside diameter of the fibers (m)
d_{mL}	Mean logarithmic diameter of fibers defined as $(d_{out}-d_{in})/\ln(d_{out}/d_{in})$ (m)
d_{out}	Outer diameter of the fibers (m)
e	Fibers thickness (m)
J_g	Total flux of glucose in the dialysis membrane process (kg/m ² s)
J_D	Flux of glucose transferred by diffusive effect (kg/s m ²)
J_C	Flux of glucose transferred by convective effect (kg/s m ²)
J_{water}	Water flux promoted by the TMP present in the system (m ³ /s m ²)
K	Overall mass transfer coefficient (m/s)
K_{UF}	Ultrafiltration coefficient reported by suppliers of dialysis membrane modules (m ³ /Pa s)
k_i	The local mass transfer coefficient for the lumen (k_L) or shell side (k_S), (m/s)
k_L	Local mass transfer coefficient in the boundary layer of the feed solution circulating in the membrane lumen side (m/s)
k_m	Local mass transfer coefficient through the liquid that fills the membrane pores (m/s)
k_S	Local mass transfer coefficient in the boundary layer of the dialysate solution circulating in the membrane shell side (m/s)
L	Fibers length (m)
N_g	Overall glucose transferred through the membrane (kg/s)
N_g^D	Glucose transferred by diffusive effect (kg/s)
N_g^C	Glucose transferred by convective effect (kg/s)
n	The total number of fibers
P	Overall permeability (m ³ /s)
Re_i	Reynolds number of the lumen (Re_L) or shell side (Re_S)
Re_L	Reynolds number of the membrane lumen side
Re_S	Reynolds number of the membrane shell side
RMS	Root mean square error (%)
Sc	Schmidt number of the aqueous phases (in this work both phases were similar to water, therefore Sc had the same value)
Sh_i	Sherwood number of the lumen (Sh_L) or shell side (Sh_S)
Sh_L	Sherwood number of the membrane lumen side
Sh_S	Sherwood number of the membrane shell side
t	time (s)
V_F	Volume of the feed tank (m ³)
v_i	Flow velocity of the solution circulating through the lumen or shell side (m/s)

separate the used enzymes from their digestion products, because it is known that the hydrolytic products generated in the GIT tend to inhibit further enzymatic hydrolysis. Hence, the use of semi-permeable membranes, acting as selective barrier, is valuable for this kind of *in vitro* intestinal systems.

Few models of the small intestine based on membrane systems have been developed. Tharakan et al. [11] fabricated an *in vitro* small intestine model (SIM) to study glucose absorption. The small intestine was simulated using an inner semi-permeable dialysis membrane and an outer flexible tube to reproduce peristalsis and segmentation motion; but no attempt was made to simulate relevant biological phenomena (e.g., intestinal pH and fluids, and body temperature). An improvement of the SIM was done by the same research group [14]. The Dynamic Duodenum (DDuo) model incorporated simulated intestinal secretions and points of pressure to reproduce segmentations and peristaltic movements. Recently, Wright and co-workers [15] developed the Human Duodenal Model (HDM) which mimics the sigmoidal shape of this first section of the small intestine, simulating the peristaltic motion by means of pneumatic movement, allowing to estimate nutrient absorption using a membrane dialysis. Other systems that simulate the coupled gastric and intestinal digestion are the *in vitro* dynamic TNO gastrointestinal model (TIM-1) [7], and the new Engineered Stomach and Small Intestine (ESIN) model [4]. Both systems use a dialysis hollow fiber membrane to simulate the passive absorption of water and digestion products in the small intestine; whereas the SimuGIT model uses a tubular ceramic microfiltration membrane for the *in vitro* absorption [16]. Although these last systems possess comparative advantages (e.g., dynamic multi-compartmental computer-controlled

models) respect to other systems, they do not shed any new light on the complex transfer processes found in absorption phenomena in the small intestine.

To provide a better understanding of the intestinal absorption phenomena, some mathematical models have been developed, where permeation of artificial membranes, as well as biological cell layers, are mainly related to passive diffusion processes [12,13]. Moser et al. [17] developed a mathematical model for the absorption/desorption process of lipophilic organic pollutants. This model assumes that the transfer across the wall of the digestive tract can be modeled as a diffusive process. Tharakan et al. [11] and Gouseti et al. [14], using an *in vitro* mechanical small intestinal model, studied the mass transfer phenomena occurring in the lumen and their potential effect on the concentration of species available for absorption. Their results suggest that nutrient absorption is controlled by mass transfer phenomena, with motion and viscosity of lumen having a strong effect on increasing and decreasing the mass transfer coefficient, respectively.

Starch is the main source of carbohydrates and energy from foods. *In vitro* starch hydrolysis has been widely studied because it can be associated with the glycemic response (GR), an indicator of postprandial glucose response for starch-based foods [18]. Several works have compared the *in vitro* starch digestion with *in vivo* blood-glucose indicators, such as GR, trying to find correlations between the fate of starch during digestion and the generation and absorption of glucose in the GIT, but discrepancies have been reported [18–22]. *In vitro* models do not resemble the physiology of the GIT, so that differences in digestion protocols can account for the lack of correlations between *in vitro* and *in vivo* tests. Argyri et al. [23] proposed a simulated

gastrointestinal digestion protocol that uses the concentration of dialyzable glucose (i.e., glucose that passes through a dialysis membrane with a molecular weight cutoff of 6–8 kDa) as a significant index for the prediction of *in vivo* responses.

1.2. Dialysis membrane process

Hollow fiber dialysis membrane process has been widely used in hemodialysis as an artificial kidney, in which the membrane acts as a separation barrier for metabolic wastes [24]. Since the used membranes are hydrophilic, the aqueous phases fill the pores (i.e. the blood and dialysate water both penetrate the membrane pores). In this regard, the driving force of the dialysis process is the concentration difference of elements mainly, between both the lumen and shell sides of the membrane. For hemodialysis, the phenomenology of the mass transfer promoted by a diffusion process has been studied by different authors [24–29], but only few works [24,29] describe an additional convective effect that promote the mass transfer, determined by a pressure difference (transmembrane pressure, TMP) between lumen and shell side, generating water or solution transfer. Thus, solute transfer through the dialysis membrane is induced by the following sequential steps (Fig. 1): (1) Solute transfer through a boundary layer of feed solution to be treated at the membrane surface; (2) Solute transfer between the feed solution at the membrane surface and the aqueous solution retained in the membrane pores; (3) Solute transfer through the aqueous solution that fills the pores; (4) Solute transfer between the aqueous solution that fills the pores at the membrane surface and the dialysate solution circulating through the shell side; (5) Mass transfer of solute into the bulk of the dialysate solution; and (6) Solute transfer promoted by the solution flow according to the TMP. Flow direction depends on the TMP value, i.e. when pressure is higher in the lumen side, this convective transfer will flow into the shell side (Fig. 1, $P_1 > P_2$).

In this work, a dialysis membrane process is used as an artificial small intestine due to its ability to simulate the diffusive transfer and absorption phenomena occurring in the small intestine, characteristics that are also complemented with the high contact area per equipment volume found when using hollow fiber membrane modules. The dialysis membrane process is the only membrane process capable of transferring solutes with high molecular weight by diffusive mass transfer, instead of micro, ultra and nanofiltration which only use the TMP as a driving

force. The objective of this work was to study the glucose transfer in an *in vitro* intestinal digestion system (i-IDS) based on dialysis membranes to simulate the glucose absorption, and also to model the mass transfer phenomena to extrapolate results of this system in the human small intestine. This work is the first comprehensive approach of this *in vitro* experimental alternative to study the glucose absorption in the human small intestine.

2. Materials and methods

2.1. Glucose solutions

Model glucose (Sigma Aldrich, USA) solutions at 15 mg/mL (83 mol/m^3) were prepared in ultrapure water (resistivity $15.0 \text{ M}\Omega \text{ cm}$) to be used as feed solutions for the simulated absorption process. This concentration is equivalent to a cup of coffee or tea with a half a sachet of sugar added, and it is also over ten times the homeostatic blood glucose level ($4\text{--}6 \text{ mol/m}^3$) found in humans [30].

2.2. Design of the *in vitro* intestinal digestion system (i-IDS)

The experimental design of the i-IDS to simulate the glucose transfer in the small intestine was divided into three zones: (i) Feed zone, (ii) Mass transfer zone, and (iii) Dialysate zone, as shown in Fig. 2. Each zone is described as follows:

- (i) Feed zone: A jacketed glass vessel (volume: 3 L) was used as feed tank. Warm water was circulated through the jacket to keep the feed at the human physiological temperature of 37°C . Glucose solution was pumped from the feed tank to the absorption zone using a peristaltic pump.
- (ii) Mass transfer zone: The absorption process was simulated by using a hemodialysis hollow fiber membrane module (Nipro, Elisio 17H-PP, USA), with a transfer area of 1.7 m^2 , inner diameter of $200 \mu\text{m}$, and pores of $40 \mu\text{m}$. The feed solution circulated through the lumen, while ultrapure water as dialysate liquid, coming from the dialysate tank, was transferred through the shell of the membrane module.
- (iii) Dialysate zone: A high density polyethylene vessel (volume: 25 L) was used as dialysate tank to supply the dialysate liquid. The same

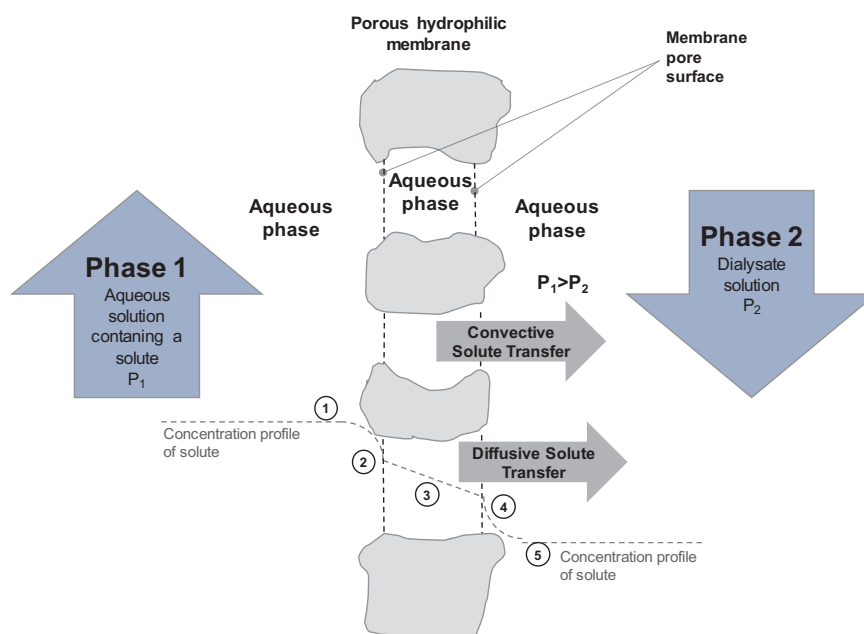


Fig. 1. Schematic representation of the mechanisms involved in the dialysis membrane process.

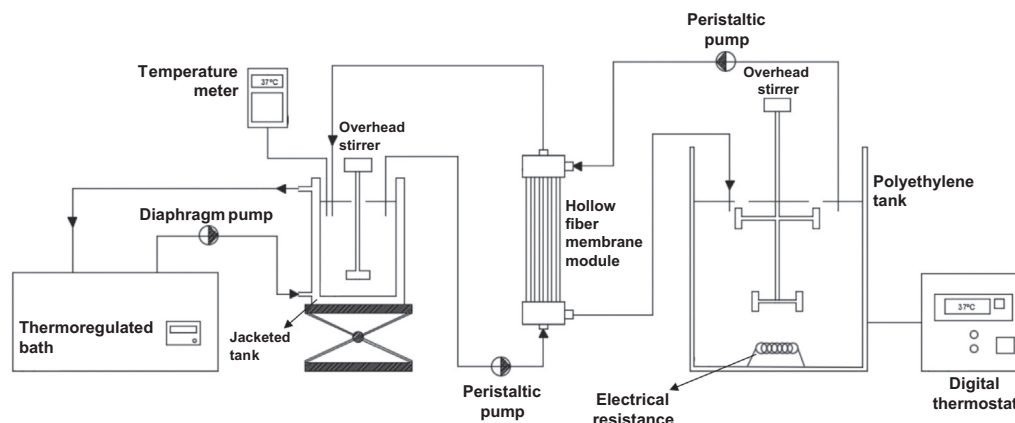


Fig. 2. Experimental scheme of the i-IDS to simulate the glucose transfer in the human small intestine.

vessel was used as dialysate sample receptor. An electrical resistance of 2000 W and a digital thermostat (STC 1000, Veto, Chile) were used to control and keep the temperature at 37 °C inside the dialysate tank. The dialysate solution was pumped from the dialysate tank to the mass transfer zone using a peristaltic pump.

2.3. Operation of the i-IDS

2.3.1. Preparation of the dialysis membrane module

In order to moisturize the hollow fibers of the dialysis membrane module, they were primed with ultrapure water prior to each experiment. Also, ultrapure water was recirculated through the lumen and shell of the membrane for 5 min, before the experimental assays. Because membranes were reused at least twice, they were washed with a 4% (v/v) solution of Germisan 430 (Difem Laboratories S.A., Chile) at the end of each assay. Germisan solution was then re-circulated through the lumen and shell for 15 min as suggested by the manufacturer.

2.3.2. Experimental assays

To evaluate the impact of the flow rate in the glucose transfer through the dialysis membrane, five assays were carried out according to the ratio of feed flow/dialysate flow: 396.6/410.4, 396.6/317.5, 396.6/250.5, 306.5/410.4 and 236.4/410.4 (nominally named as 400/410, 400/300, 400/250, 300/410 and 200/410, respectively). For each experiment, the feed tank was filled with 2 L of glucose solution (C_g^F), while the dialysate tank was filled with 20 L of ultrapure water (C_g^D), assuring a ratio of feed volume/dialysate volume of 1:10 which allows to generate the required driving force induced by the glucose concentration gradient between the bulk of the feed and dialysate phases. The feed flow circulated through the membrane lumen side, and dialysate solution was fed into the shell side of the membrane module. Both tanks were maintained at 37 ± 1 °C during the assays. In order to determine the glucose concentration in each tank during the process time, each test was carried out during 1 h, simultaneously taking aliquots (2 mL) from both the feed and the dialysate tanks. During the first 20 min of the experiment, the aliquots were taken at intervals of 2 min and then at intervals of 5 min until completing 1 h of assay. In addition, the volume of both tanks was registered during the assays. The experimental conditions and membrane characteristics are summarized in Table 1. All experiments were done in triplicate and results are presented as mean values with standard deviations.

2.3.3. Glucose concentration measurements

Glucose concentration in the feed and dialysate tanks was determined using a spectrophotometric method for the analysis of reducing sugars (Miller's technique) with the 3,5 dinitrosalicylic acid (DNS) [31,32]. The absorbance of solutions was measured by an UV–vis

spectrophotometer (Shimadzu Corporation, UV mini-1240, Japan) at 600 nm.

2.4. Dialysis membrane process and phenomenological approach

Mass transfer of glucose from the feed solution into the dialysate solution is determined by the difference of chemical potentials between feed solution and dialysate solution, expressed as the difference of concentration (diffusive effect) and transmembrane pressure (convective effect) [24,29]. Hence, the glucose transfer (J_g) in the dialysis membrane process can be presented as follows:

$$J_g = J_D + J_C \quad (1)$$

The transfer of glucose promoted by diffusion can be estimated by a glucose concentration gradient between both phases, and a mass transfer coefficient. Thus, the glucose transfer rate by diffusive effect can be described as:

$$J_D = K(C_g^F - C_g^D) \quad (2)$$

Eq. (2) can be rewritten to estimate the glucose transferred by diffusive effect in the following equation:

Table 1
Experimental conditions of the i-IDS and membrane characteristics.

Description	Value	Unit
Feed tank volume	3.0	L
Dialysate tank volume	25.0	L
Feed solution volume	2.0	L
Dialysate water volume	20.0	L
Feed solution flow	236.6–396.6	L/min
Feed flow/Dialysate flow ratio ^a	396.6/410.4; 396.6/317.5; 396.6/250.5; 306.5/410.4; 236.4/410.4	mL/mL
Temperature	37.0	°C
Glucose concentration in the feed solution	83	mol/m ³
Membrane material	Polyethersulfone	–
Number of fibers	9984	–
Surface contact area	1.7	m ²
Fiber outer diameter	280	μm
Fiber inside diameter	200	μm
Shell inside diameter	0.036	m
Membrane contactor length	0.271	m
Porosity ^b	0.38	–
K_{UF}	74	mL/h/mmHg
Module model	Elisio 170H	–

^a The feed flow/dialysate flow ratio were nominally named as 400/410, 400/300, 400/250, 300/410 and 200/410.

^b Porosity was measured by using a gravimetric method [45,46].

$$N_g^D = K A_T \Delta C_g \tag{3}$$

The overall mass transfer coefficients are widely used to estimate mass transfer of solutes by the incorporation of the mass transfer resistance concept, particularly for hollow fibers membrane contactor processes [33]. Thus, the overall mass transfer coefficient can be represented as a global resistance (see Eq. (10), Appendix A).

The resistances-in-series mass transfer model is useful for processes where the determination of concentrations at the interface is complex. This model has been applied in different membrane separation processes. For example, in cyanide recovery, when a gas filled membrane absorption process [34] or supercritical separation of fluids are used in membrane contactors [35].

The local mass transfer coefficient at the feed solution boundary layer in Eq. (10) can be estimated by a specific correlation [36,37], which considers the geometry and the dimensionless Reynolds (Re),

Schmidt (Sc) and Sherwood (Sh) numbers of the system. In this study, the feed solution was circulating on the membrane lumen side, and the dialysate solution was circulating on the membrane shell side. The mass transfer coefficient of the liquid feed boundary layer can be estimated by the Yang and Cussler model [38] (see Eq. (11), Appendix A).

On the other hand, the mass transfer coefficient of the dialysate solution boundary layer can be estimated by the Gawronski and Wrzesinska correlation [39], which fits with the operational conditions performed in this work, correctly representing the hydrodynamic conditions of the membrane module (see Eq. (12), Appendix A).

The estimation of the local mass transfer coefficients requires determination of the physical properties of both liquid phases. These physical properties can be estimated by empirical and semi-empirical models dependent on the operational conditions of the system. Thus, experimental data of density and viscosity for the water phase can be obtained from Green and Perry [40], which have been correlated as a

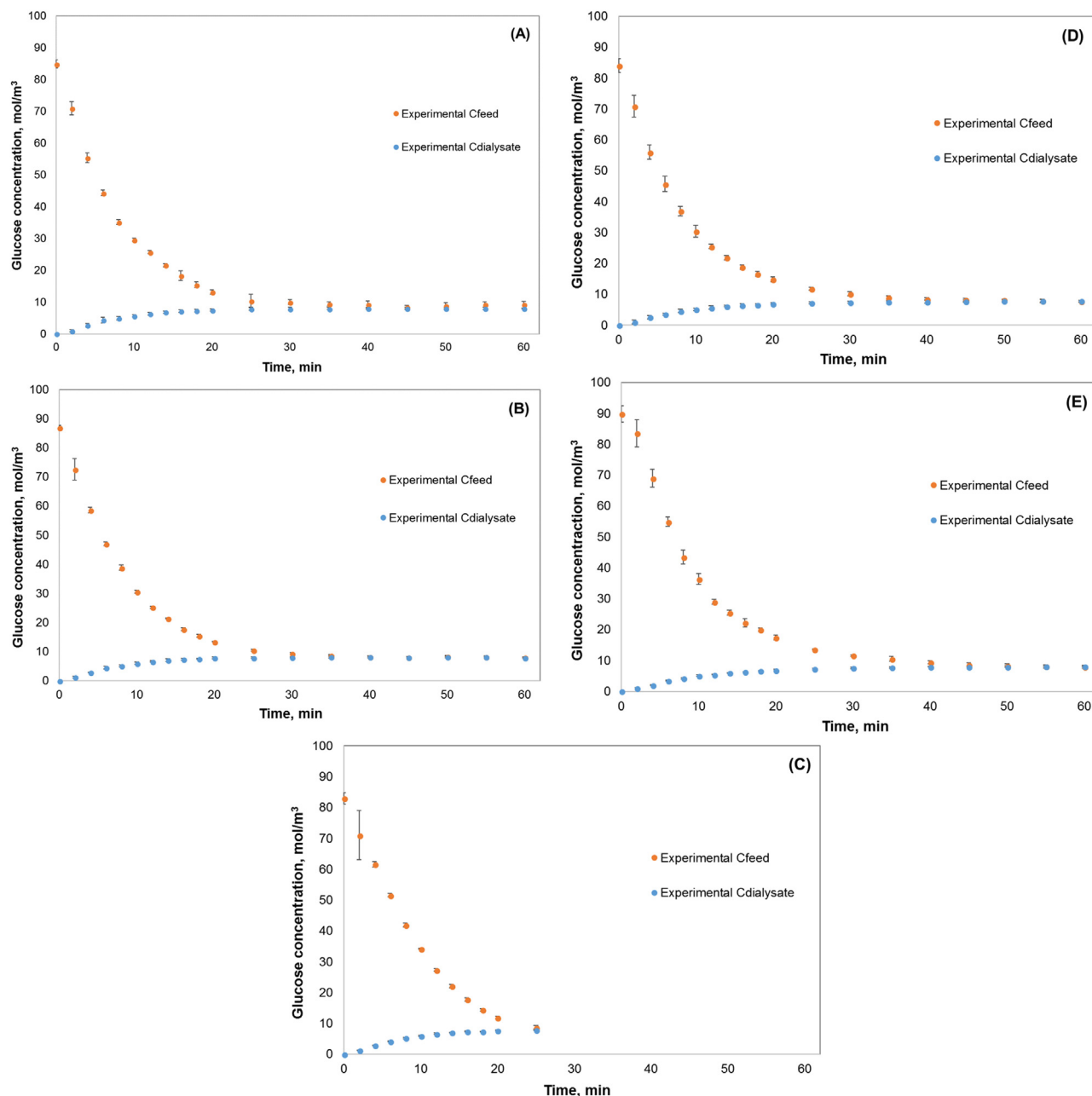


Fig. 3. Experimental profiles of glucose concentration in the feed and dialysate tanks for different feed flow/dialysate flow ratios: (A) 400/410, (B) 400/300, (C) 400/250, (D) 300/410, (E) 200/410.

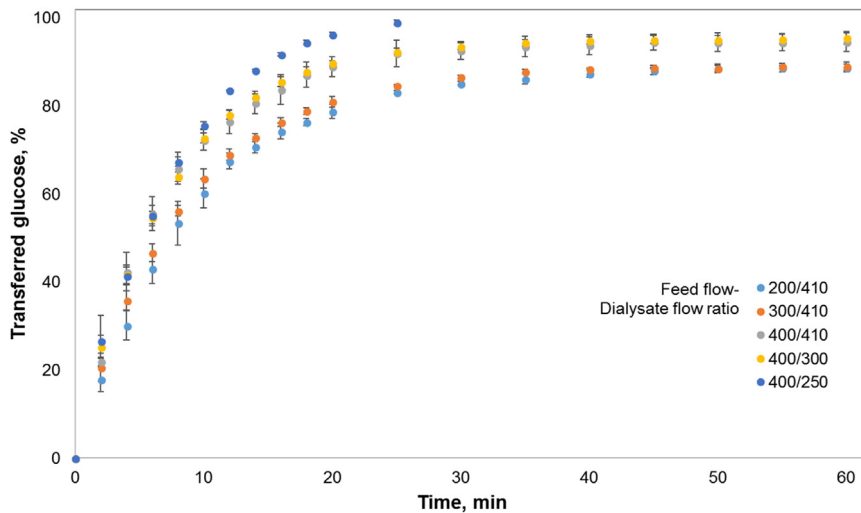


Fig. 4. Percentage of transferred glucose for different feed flow/dialysate flow ratios.

function of temperature by Estay et al. [35].

The value of the glucose diffusion coefficient in water can be estimated from experimental data dependent on water temperature and viscosity, based on the Stokes-Einstein's equation [37]. Data of the glucose diffusion coefficient in water were obtained from Cengel [41], who reported a value of $0.69 \times 10^{-5} \text{ cm}^2/\text{s}$ at 25 °C. Considering this value, the glucose diffusion coefficient in water for different conditions can be then estimated by Eq. (17) (see Appendix A).

On the other hand, the glucose transfer by convective effect is promoted by the water transfer determined by the TMP according to [27].

$$J_{water} = K_{UF} \Delta P \tag{4}$$

The convective flow of water transports glucose has then the same concentration of the respective phase. Therefore, the convective flow of glucose will depend on the water flow transferred, which in turn, will be limited by glucose concentration in the receiving phase. The following expression can be applied to estimate the convective transfer of glucose.

$$J_C = N_g^C = K_{UF} \Delta P \Delta C_g \tag{5}$$

Replacing the Eqs. (5) and (3) in the Eq. (1), it is possible to estimate the overall glucose transfer by combining the diffusive and convective effects, according to:

$$N_g = (KA_T + K_{UF} \Delta P) \Delta C_g \tag{6}$$

This last equation describes the transferred glucose through the membrane, which can be applied to quantify the diffusive and convective effects that govern the process. From this equation, it is also possible to combine the parameters $KA_T + K_{UF} \Delta P$ with the purpose of determining the overall permeability ($P, \text{ m}^3/\text{s}$) of the membrane.

The Eq. (6) can be used in a non-stationary mass balance of glucose in the system, in agreement with the experimental conditions assessed in this work (Fig. 2), with the aim of obtaining a phenomenological approach for the glucose transfer including diffusive and convective effects:

$$\ln \left(\frac{C_g^F - C_g^D}{C_g^0 - C_g^D} \right) = - \left(KA_T + K_{UF} \Delta P \right) \frac{t}{V_F} \tag{7}$$

Thus, Eq. (7) allows estimating the glucose concentration profile for each time of the dialysis extraction process. This model considers the following main assumptions:

- The glucose concentration profile does not suffer variations along the length of the membrane module for each process time.
- The glucose concentration in the dialysate phase is the same for each process time.

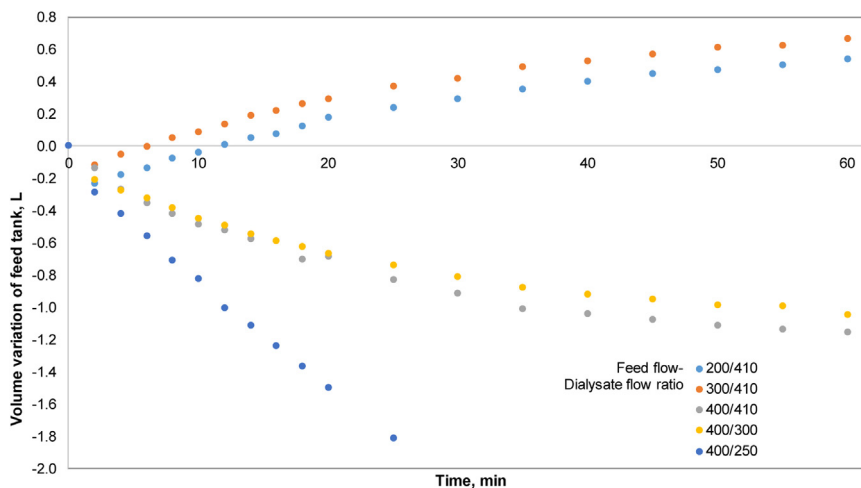


Fig. 5. Cumulative water flow and transferred into and from dialysate solution (positive curves correspond to the water flow from the dialysate solution into the feed solution and vice versa).

Table 2
Estimated parameters from the simulation of the phenomenological models.

Parameter	Feed flow-Dialysate flow ratio				
	400/410	400/300	400/250	300/410	200/410
ϕ	0.604	0.604	0.604	0.604	0.604
Velocity of lumen side, m/s	0.021	0.021	0.021	0.016	0.013
Velocity of shell side, m/s	0.017	0.013	0.010	0.017	0.017
Re_L	6.07	6.07	6.07	4.69	3.62
Re_S	4.43	3.42	2.7	4.43	4.43
k_L , m/s	1.27×10^{-5}	1.27×10^{-5}	1.27×10^{-5}	1.16×10^{-5}	1.07×10^{-5}
k_S , m/s	5.14×10^{-6}	4.29×10^{-6}	3.63×10^{-6}	5.14×10^{-6}	5.14×10^{-6}
k_m , m/s	4.36×10^{-6}	4.36×10^{-6}	4.36×10^{-6}	4.36×10^{-6}	4.36×10^{-6}
K , m/s	2.43×10^{-6}	2.28×10^{-6}	2.13×10^{-6}	2.39×10^{-6}	2.35×10^{-6}
TMP ^a , mmHg	19.66	18.45	59.73	− 9.97	− 7.25
Mass transfer resistance of lumen side, %	19.2	18.0	16.8	20.6	22.0
Mass transfer resistance of shell side, %	33.8	38.0	42.0	33.3	32.7
Mass transfer resistance of membrane, %	47.0	44.0	41.2	46.2	45.3

^a TMP was estimated from the water flows measured in test-work (Fig. 5). This value corresponds to the mean TMP for each feed flow/dialysate flow ratio.

- There are no reactive phenomena in this system. Further studies should include a reactive effect during dialysis process, in order to simulate the enzyme reactive behavior found in the human small intestine.

The two first assumptions regarding the glucose concentration can be conducted by using a mean logarithmic glucose concentration in Eq. (6), described as:

$$N_g = (KA_T + K_{UF} \Delta P) \Delta C_{mlg} \quad (8)$$

Thus, Eqs. (6) and (8) can be combined with a steady-state glucose mass balance in the dialyzer for each process time in order to obtain the C_g^F profile.

The phenomenological approach was used to scale-up the human small intestine conditions to the operational parameters of the i-IDS (artificial small intestine). This means that when using the i-IDS is possible to represent the absorption performance of the human small intestine according to fixed experimental parameters. The phenomenological approach involves two models based on Eqs. (1)–(18), which were developed by a numerical algorithm that estimates the transferred glucose from the feed solution into the dialysate solution. Both models estimate the physical properties of water for both feed and dialysate solutions (density and viscosity) and diffusion coefficient (Eq. 17). In addition, both models estimate the dimensionless numbers of Sh , Re and Sc , and the respective mass transfer coefficients. Furthermore, the transmembrane pressure was estimated using the experimental results of water flow for each feed flow/dialysate flow ratio assessed.

In terms of simulation, both models were defined as Model 1 and Model 2. Model 1 estimates the glucose concentration profile with respect to time using Eq. (7). Instead, Model 2 estimates the glucose concentration profile using Eq. (8) and then comparing the value obtained from these equations with those obtained from a glucose mass balance to the dialyzer. When the difference between the transferred glucose values is lower than the set target, the iterative routine was finished.

Simulations of both models were carried out by comparing their results with the experimental glucose concentration profiles. All simulations were performed at same experimental conditions studied in this work. Finally, the model that presented a better adjustment with experimental results obtained from the i-IDS was compared and scaled-up to the human small intestine conditions, in order to propose experimental operational conditions of the i-IDS that simulate the absorption process in the human small intestine. The adjustment of the experimental data to the models was estimated by nonlinear regression, using as an objective the function of the root mean square error (RMS) minimization, defined as follows:

$$\% \text{ RMS} = \left(\frac{1}{n} \sum_{i=1}^n \left(\frac{\text{Value}_{\text{experimental}} - \text{Value}_{\text{fit}}}{\text{Value}_{\text{experimental}}} \right)^2 \right)^{0.5} \times 100\% \quad (9)$$

3. Results and discussion

3.1. Glucose concentration profiles in the i-IDS under different operational conditions

Experimental results of the glucose concentration profiles in the feed and dialysate tanks with respect to time under different ratios of feed flow/dialysate flow are shown in Fig. 3. For all the experimental conditions, while the glucose concentration in the feed tank decreased, the one in the dialysate tank increased, reaching similar values. With these results, it is important to mention that the glucose transfer is mainly promoted by the difference of glucose concentration between both sides of membrane. The contribution to mass transfer by different effects (diffusive and convective) is quantified in Section 3.2. In this context, the design and operation of the i-IDS was correct in terms of defining the dialysate solution volume (20 L) with respect to the feed solution volume (2 L), which allowed to generate the required driving force induced by the concentration gradient (difference of glucose concentration) to promote the glucose transfer in the system.

The glucose concentration in the dialysate tank reached values around 8–9 mol/m³, determining a glucose transfer in around 90% for each experimental condition assessed (Fig. 4). This final value of glucose transfer was achieved at different times, according to the feed flow/dialysate flow ratio. When the dialysate flow was higher than the feed flow (experimental cases 200/410 and 300/410), the 90% of transferred glucose was achieved at times close to 60 min. Instead, the glucose transfer reached values close to 90% at 15–20 min when the feed flow/dialysate flow ratio was close or over 1.0 (cases 400/410, 400/300 and 400/250). These differences could be explained by the convective transfer of glucose promoted by the TMP generated between both sides of the membrane. This TMP was generated by both the pressure drop along to the module in each side of the membrane and the variation of tanks level – changing the hydrostatic pressure in the pumps - promoted by the convective transfer of the solution as described in equation (12) (Fig. 5). Even though the glucose transfer is mainly induced by diffusion (results shown in Section 3.2), the convective flow determines the solution transfer affecting the TMP in the system. These results demonstrate the ability of the i-IDS to simulate the glucose transfer by reaching similar values of absorption, just as found in the human small intestine (~ 96%) [42]. Also, the i-IDS is a highly flexible experimental prototype able to change operational conditions to predict absorption values in the human small intestine. However, the

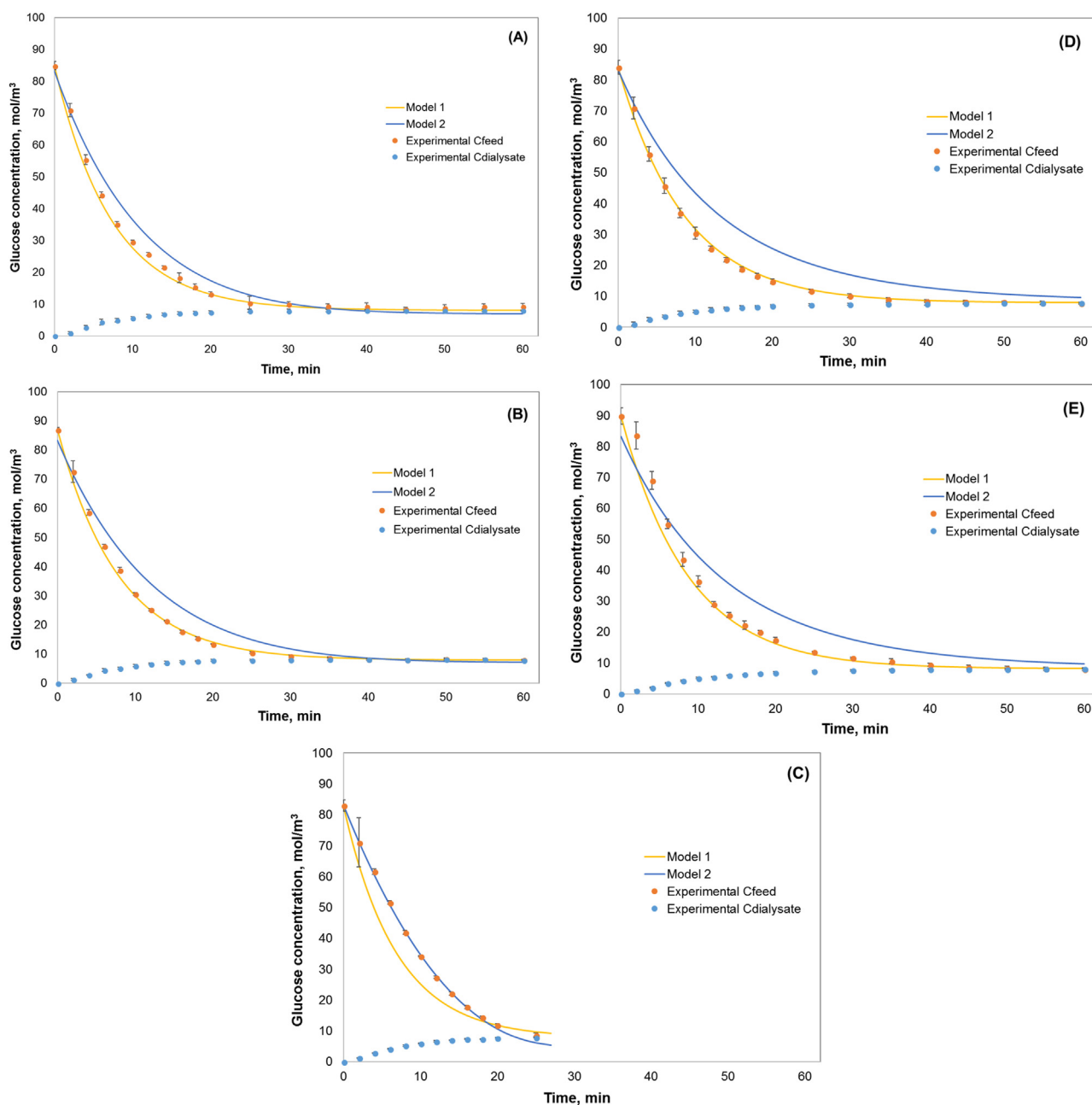


Fig. 6. Profiles of glucose concentration in the feed and dialysate tanks for different feed flow/dialysate flow ratios: (A) 400/410, (B) 400/300, (C) 400/250, (D) 300/410, (E) 200/410. Symbols show the experimental data while lines represent the results obtained from the models 1 and 2 for the glucose concentration in the feed tank.

Table 3

RMS values between experimental data and results obtained from the phenomenological models.

RMS, %	Feed flow-Dialysate flow ratio				
	400/410	400/300	400/250	300/410	200/410
Model 1	7.51	3.73	18.56	3.21	7.11
Model 2	20.51	27.65	9.20	49.75	35.89

presence of convective and diffusive processes during the glucose transfer in the i-IDS makes it difficult to interpret results, particularly when it comes to scale-up the conditions found in the human small intestine. This issue forces the development of phenomenological models when comparing and extrapolating data from experimental

Table 4

Quantification of the convective effect in the glucose transfer in the i-IDS.

Convective effect	Feed flow-Dialysate flow ratio				
	400/410	400/300	400/250	300/410	200/410
Percentage of glucose transferred by convective effect	8.9	8.9	25.3	- 5.3	- 3.9

system to the human small intestine. This is a remarkable fact considering that the majority of studies based on *in vitro* intestinal models do not deepen our understanding of the role of the mass transfer phenomena (*i.e.*, diffusion and convection) in absorption outcomes.

Table 5
Results of scaling-up of the i-IDS to the human small intestine using Model 1.

Parameter	Human small intestine	Feed flow-Dialysate flow ratio				
		400/410	400/300	400/250	300/410	200/410
Glucose Transfer, %	96.4 ^a	23.75 ^b	23.75 ^b	23.75 ^b	23.75 ^b	23.75 ^b
C_g^O , mg/mL	15	15	15	15	15	15
C_g^F , mg/mL	0.54	11.385	11.385	11.385	11.385	11.385
C_g^D , mg/mL	0	1.4 ^c	1.4 ^c	1.4 ^c	1.4 ^c	1.4 ^c
V_F , L	0.5 ^d	2	2	2	2	2
N_g^e , g	7.23	7.23	7.23	7.23	7.23	7.23
t , min	180	2.3 ^b	2.4 ^b	2.1 ^b	2.7 ^b	2.7 ^b
A_T , m ^b	30 ^f	1.7	1.7	1.7	1.7	1.7
K , m/s	–	2.43×10^{-6}	2.28×10^{-6}	2.13×10^{-6}	2.39×10^{-6}	2.35×10^{-6}
TMP, mmHg	–	19.66	18.45	59.73	– 9.97	– 7.25
Overall permeability ($K_A + K_{UF}TMP$) ^g , m ³ /s	1.54×10^{-7}	4.54×10^{-6}	4.26×10^{-6}	4.86×10^{-6}	3.86×10^{-6}	3.85×10^{-6}
Feed flow, mL/min	3 ^h	400	400	400	300	200

^a Value of glucose transfer reported in literature [42].

^b Prototype recoveries and time were estimated from the model 1 to fit the N_g value estimated for the small intestine human.

^c Average value obtained for dialysate glucose concentration in the experimental runs.

^d The stomach volume was defined as an average value of those reported in literature [8,10,47].

^e The N_g value was estimated using a mass balance according to: $N_g = V_F C_g^O (1-Rec/100)$.

^f Value of the small intestine transfer area reported in literature [48].

^g The overall permeability ($K_A + K_{UF}TMP$) was estimated from the model 1 for the human small intestine, while it was directly estimated from the mass transfer parameters for the experimental prototype.

^h Value of the flow fed into the small intestine reported in literature [49–51].

3.2. Validation and simulation results of the phenomenological approach

The two phenomenological models previously described (Section 1.2) were analyzed using the operational parameters shown in Table 1. Likewise, Table 2 presents the parameters values estimated for both models. These results indicate that the membrane (termed “mass transfer zone”) was the controlling stage of the mass transfer by diffusive effect, in the process, although the mass transfer resistances of the lumen and shell side represented the 55–60% of the overall mass transfer resistances. In addition, the TMP values were based on the water flows reported in an earlier section (Fig. 5), determining its magnitude and direction (negative for the water transfer into the feed solution, and positive for the water transfer into the dialysate solution). The values reported in Table 2 are the base for the glucose concentration profiles results shown in Fig. 6. According to these results, both phenomenological models fit with the experimental results; however, Model 1 presented %RMS values lower than 18.6%, as shown in Table 3. These results could be unexpected, since Model 2 includes the effect of module length in the glucose concentration profile and the variation of glucose concentration in the dialysate. This behavior could be explained by the fit of the Gawronski and Wrzesinska's correlation [39] for the glucose transfer by diffusive effect, although the results of the convective effect shown in Table 4 indicate that the fit of the Model 2 to the experimental data increases when the diffusive effect has decreased. Therefore, the glucose transfer by convective effect is more influenced by the changes produced along the module with respect to the diffusive effect. Hence, Model 1 - simpler than Model 2 - can be used for a feed flow/dialysate flow ratio close to 1.0, whereas model 2 should be used when this ratio is far from 1.0.

A final estimation to scale-up the results from this study with the realistic conditions of the human small intestine was performed. The scaling-up procedure is a critical step to extrapolate future experimental results from the operation of the i-IDS to the human small intestine. With this in mind, Table 5 shows the scaling-up results, where the i-IDS reached the mass of glucose transferred in the human small intestine in a time ranging between 2 and 3 min. Instead the 180 min reported for the human small intestine reached the same value (7.23 g, value estimated as described in Table 5). This difference in the processing time is explained by the high feed flows used when operating the i-IDS (200–400 mL/min) with respect to the conditions found in the human

small intestine (3 mL/min) [8]. The higher feed flows used in the i-IDS determined the increase in the overall permeability of the membrane (from 1.54×10^{-7} to around 4.0×10^{-6} m³/s), increasing the overall kinetic of the process from 180 to 2 min.

Notwithstanding the above results, the processing times studied with the i-IDS could be modified according to the chosen nutrient (solute) to be extracted or transferred in this system. For this purpose, some experimental adjustments could be addressed in order to promote a slower extraction process. For example, the use of a dialyzer with a lower area and smaller membrane pore size, the operation at lower feed flow/dialysate flow ratio, or the use of a higher dialysate solute concentration. However, these adjustments should be implemented after testing and modeling the process, but now also including the reactive effects present in the human small intestine.

On the other hand, the use of dialysis membranes to study glucose available for absorption has been previously reported. The quantification of the overall permeability of the small intestine, in terms of effective permeability, was performed by Wright et al. (2016) [15], using an experimental duodenum prototype. These authors found lower values (3.27×10^{-3} L/cm h, equivalent to 5.2×10^{-8} m³/s according to the length used by them) than those estimated in this study (3.85 – 4.86×10^{-6} m³/s, Table 5). The value of effective permeability obtained by Wright and co-workers [15] was compared to *in vivo* results (1.0×10^{-3} L/cm h, equivalent to 1.6×10^{-8} m³/s) found by Fine et al. [43], who conducted *in vivo* test on intestinal permeability of humans. These results show lower values of overall permeabilities than the estimated ones in this work due to hydrodynamic differences among the experimental systems. However, the experimental and theoretical methodology here presented allows to predict nutrient transference in the human small intestine. Further studies, including the reactive effect, will be relevant to move along in the understanding and prediction of *in vitro* systems of the human small intestine.

Based on the same purpose, Tharakan et al. [11] and Gouseti et al. [14] studied mass transfer using a model of small intestine based on a mono-tubular semi-permeable membrane dialysis module. These studies were focused on describing the hydrodynamic conditions in the lumen side of the simulated small intestine. The values of the overall mass transfer coefficients obtained from these studies (ranging from 3.2×10^{-7} to 5.35×10^{-7} m/s) are lower than the overall permeability of the human small intestine predicted in this work (Table 5)

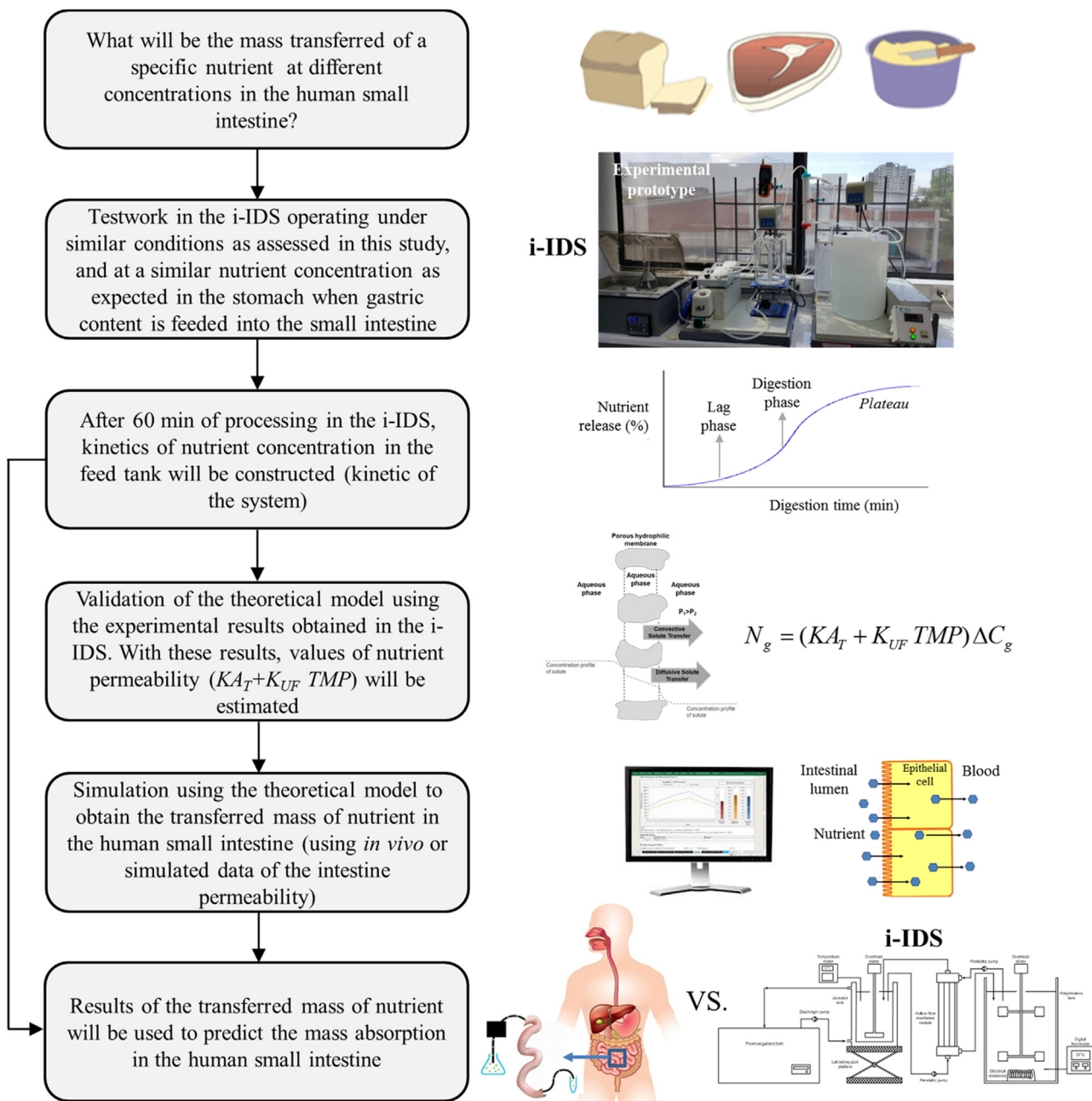


Fig. 7. Flow chart describing the theoretical and experimental methodology to quantify and predict nutrient absorption in the human small intestine using the i-IDS.

($1.54 \times 10^{-7} \text{ m}^3/\text{s}$, with respect to the equivalent 1.51×10^{-8} to $2.52 \times 10^{-8} \text{ m}^3/\text{s}$ estimated by these authors according to the length and area used in their studies). The differences found among these results may be due to some drawbacks associated with the model proposed by these authors, such as: (i) the model developed did not include the convective transfer and reactive effects, (ii) the estimation of mass transfer coefficients in the lumen, membrane, and shell sides was based on experimental results, and (iii) the experimental results of the mass transfer coefficient in the lumen side were fitted with results obtained from a correlation for turbulent regime, when Re values were less than 1.0 (laminar regime). Despite these limitations, the model developed by Tharakan et al. [11] and Gouseti et al. [14] could be considered a first interesting contribution to the research discussion regarding the estimation and understanding of the mass transfer in the human small intestine. However, it is restricted in its applicability to predict the mass transfer of different nutrients in the small intestine, since the theoretical

understanding of the system is limited.

Finally, and as it was mentioned earlier, the *in vitro* digestion models have advantages: they are easy-to-use, fast, economic, they could lead to useful information on trends, and they are also designed for formulation screening. However, some disadvantages are: How realistic are they? How can models be adapted for different systems? Is there a standard method possible? How is it possible to obtain useful information of mechanism of nutrient absorption? Is there an agreement between *in vitro* and *in vivo* measures? In trying to answer at least some aspects related to these last two questions, it could be useful to compare the *in vitro* results for the transferred glucose in this work with *in vivo* data reported by previous studies. Blackburn and co-workers [44] carried out experiments in ten human volunteers to analyze intestinal absorption of glucose by means of a steady-state perfusion technique. Glucose solutions (15 and 30 mmol/L) were continuously infused at a steady rate of 10 mL/min, obtaining values of glucose absorption

ranging from 6 to 18 mmol/h in a length of 25 cm of small intestine, values that were equivalent to a range of about 255–764 mmol/h m². In the case of the present study, the glucose absorption fluctuated between the estimated values of 525 and 600 mmol/h m², considering the following experimental and theoretical parameters: $N_g = 7.23$ g; $t_{absorption} = 2.3$ – 2.7 min; $A_T = 1.7$ m². It is clear, in these circumstances, that the results of glucose absorption obtained in this work are in agreement with those found in human studies. Bearing this in mind, it is possible to establish that the design and operation of the i-IDS, and the phenomenological model (Model 1) developed in this study, were able to simulate realistic absorption values for glucose, just as they occur in the human small intestine. This issue is the main contribution of the present work: a comprehensive experimental and theoretical methodology able to extrapolate or predict the absorption performance of different nutrients in the human small intestine (Fig. 7), but interpretation of results must be done carefully, because human digestion is indeed a complex process. Future work must be geared towards the designing of more realistic *in vitro* intestinal models that simulate nutrient digestion and absorption, where a phenomenological understanding of the mass transfer processes involved in these systems is definitely needed as well.

4. Conclusions

This work aimed at proposing a first experimental and

Appendix A

$$\frac{1}{K} = \frac{1}{k_L} + \frac{d_{in}}{k_m d_{ml}} + \frac{d_{in}}{k_S d_{out}} \quad (10)$$

$$Sh_L = 1.64 \left(Re_L Sc \frac{d_{in}}{L} \right)^{1/3} \quad (11)$$

$$Sh_S = 0.09 (1 - \phi) Re_S^{(0.8 - 0.16\phi)} Sc^{1/3} \quad (12)$$

$$Sh_i = \frac{k_i D_{glucose-water}}{CL} \quad (13)$$

$$Re_i = \frac{\rho_{water} v_i CL}{\mu_{water}} \quad (14)$$

$$Sc = \frac{\mu_{water}}{\rho_{water} D_{glucose-water}} \quad (15)$$

$$k_m = \frac{D_{glucose-water} \varepsilon}{\tau e} \quad (16)$$

$$\frac{D_{glucose-water}(T_A)}{D_{glucose-water}(T_B)} = \frac{T_A \mu_B}{T_B \mu_A} \quad (17)$$

$$\Delta C_{m \lg} = \frac{(C_g^F - C_g^D)_1 - (C_g^F - C_g^D)_2}{\ln \left[\frac{(C_g^F - C_g^D)_1}{(C_g^F - C_g^D)_2} \right]} \quad (18)$$

References

- [1] E. Troncoso, J.M. Aguilera, Food microstructure and digestion, *Food Sci. Technol.* 23 (2009) 30–33.
- [2] M.J.S. Wickham, R.M. Faulks, J. Mann, G. Mandalari, The design, operation, and application of a dynamic gastric model, *Dissolution Technol.* 19 (2012) 15–22, <https://doi.org/10.14227/DT190312P15>.
- [3] O. Menard, T. Cattenoz, H. Guillemin, I. Souchon, A. Deglaire, D. Dupont, D. Pique, Validation of a new *in vitro* dynamic system to simulate infant digestion, *Food Chem.* 145 (2014) 1039–1045, <https://doi.org/10.1016/j.foodchem.2013.09.036>.
- [4] A. Guerra, S. Denis, O. LeGoff, V. Sicardi, O. Francois, A.F. Yao, G. Garranti, A.P. Manzi, E. Beyssac, M. Alric, S. Blanquet-Diot, Development and validation of a new dynamic computer-controlled model of the human stomach and small intestine, *Biotechnol.* 113 (2016) 1325–1335, <https://doi.org/10.1002/bit.25890>.
- [5] S. Marze, Bioavailability of nutrients and micronutrients: advances in modeling and *in vitro* approaches, *Annu. Rev. Food Sci. Technol.* 8 (2017) 35–55, <https://doi.org/10.1146/annurev-food-030216-030055>.
- [6] K. Venema, R. Havenaar, M. Minekus, Improving *in vitro* simulation of the stomach and intestines, in: D.J. McClements, E.A. Decker (Eds.), *Des. Funct. Foods Meas. Control. Food Struct. Break. Nutr. Absorpt.* CRC Press, Boca Raton, FL, 2009, pp. 314–339.
- [7] M. Verwei, M. Minekus, E. Zeijdner, R. Schilderink, R. Havenaar, Evaluation of two

- dynamic in vitro models simulating fasted and fed state conditions in the upper gastrointestinal tract (TIM-1 and tiny-TIM) for investigating the bioaccessibility of pharmaceutical compounds from oral dosage forms, *Int. J. Pharm.* 498 (2016) 178–186, <https://doi.org/10.1016/j.ijpharm.2015.11.048>.
- [8] F. Kong, R.P. Singh, A human gastric simulator (HGS) to study food digestion in human stomach, *J. Food Sci.* 75 (2010) E627–E635, <https://doi.org/10.1111/j.1750-3841.2010.01856.x>.
- [9] H. Kozu, Y. Nakata, M. Nakajima, M. Neves, K. Uemura, S. Sato, I. Kobayashi, S. Ichikawa, Development of a human gastric digestion simulator equipped with peristalsis function for the direct observation and analysis of the food digestion process, *Food Sci. Technol. Res.* 20 (2014) 225–233, <https://doi.org/10.3136/fstr.20.225>.
- [10] L. Barros, C. Retamal, H. Torres, R.N. Zúñiga, E. Troncoso, Development of an in vitro mechanical gastric system (IMGS) with realistic peristalsis to assess lipid digestibility, *Food Res. Int.* 90 (2016) 216–225, <https://doi.org/10.1016/j.foodres.2016.10.049>.
- [11] A. Tharakan, I.T. Norton, P.J. Fryer, S. Bakalis, Mass transfer and nutrient absorption in a simulated model of small intestine, *J. Food Sci.* 75 (2010) E339–E346, <https://doi.org/10.1111/j.1750-3841.2010.01659.x>.
- [12] M. Kansy, F. Senner, K. Gubernator, Physicochemical high throughput screening: parallel artificial membrane permeation assay in the description of passive absorption processes, *J. Med. Chem.* 41 (1998) 1007–1010, <https://doi.org/10.1021/jm970530e>.
- [13] E. Le Ferrec, C. Chesne, P. Artusson, D. Brayden, G. Fabre, P. Gires, F. Guillon, M. Rousset, W. Rubas, M.L. Scarino, In vitro models of the intestinal barrier, *Altern. Lab. Anim.* 29 (2001) 649–668.
- [14] O. Gouseti, M.R. Jaime-Fonseca, P.J. Fryer, C. Mills, M.S.J. Wickham, S. Bakalis, Hydrocolloids in human digestion: dynamic in-vitro assessment of the effect of food formulation on mass transfer, *Food Hydrocoll.* 42 (2014) 378–385, <https://doi.org/10.1016/j.foodhyd.2014.06.004>.
- [15] N.D. Wright, F. Kong, B.S. Williams, L. Fortner, A human duodenum model (HDM) to study transport and digestion of intestinal contents, *J. Food Eng.* 171 (2016) 129–136, <https://doi.org/10.1016/j.jfoodeng.2015.10.013>.
- [16] E. Rivas-Montoya, J.M. Ochando-Pulido, A. Martínez-Férez, Application of a novel gastrointestinal tract simulator system based on a membrane bioreactor (SimuGIT) to study the stomach tolerance and effective delivery enhancement of nanoencapsulated macelignan, *Chem. Eng. Sci.* 140 (2016) 104–113, <https://doi.org/10.1016/j.ces.2015.10.006>.
- [17] G.A. Moser, M.S. McLachlan, Modeling digestive tract absorption and desorption of lipophilic organic contaminants in humans, *Environ. Sci. Technol.* 36 (2002) 3318–3325, <https://doi.org/10.1021/es015853l>.
- [18] P.A. Magallanes-Cruz, P.C. Flores-Silva, L.A. Bello-Pérez, Starch structure influences its digestibility: a review, *J. Food Sci.* 82 (2017) 2016–2023, <https://doi.org/10.1111/1750-3841.13809>.
- [19] J. Hasjim, G. Cesbron Lavau, M.J. Gidley, R.G. Gilbert, In vivo and in vitro starch digestion: are current in vitro techniques adequate? *Biomacromolecules* 11 (2010) 3600–3608, <https://doi.org/10.1021/bm101053y>.
- [20] A. Ferrer-Mairal, C. Peñalva-Lapuente, I. Iglesia, L. Ustasun, P. De Miguel-Etayo, S. Remón, E. Cortés, L.A. Moreno, In vitro and in vivo assessment of the glycemic index of bakery products: influence of the reformulation of ingredients, *Eur. J. Nutr.* 51 (2012) 947–954, <https://doi.org/10.1007/s00394-011-0272-6>.
- [21] C.T. Vangsoe, A.K. Ingerslev, P.K. Theil, M.S. Hedemann, H.N. Laerke, K.E. Knudsen, In vitro starch digestion kinetics of diets varying in resistant starch and arabinoxylan compared with in vivo portal appearance of glucose in pigs, *Food Res. Int.* 88 (2016) 199–206, <https://doi.org/10.1016/j.foodres.2016.02.005>.
- [22] T.M.S. Wolever, B.-W. van Klinken, N. Bordenave, M. Kaczmarczyk, A.L. Jenkins, Y.F. Chu, Reformulating cereal bars: high resistant starch reduces in vitro digestibility but not in vivo glucose or insulin response; why protein reduces glucose but disproportionately increases insulin, *Am. J. Clin. Nutr.* 104 (2016) 995–1003, <https://doi.org/10.3945/ajcn.116.132431>.
- [23] K. Argyri, A. Athanasatou, M. Bouga, M. Kapsokelafou, The potential of an in vitro digestion method for predicting glycemic response of foods and meals, *Nutrients* 8 (2016) 1–12, <https://doi.org/10.3390/nu8040209>.
- [24] A.P. Broek, H.A. Teunis, D. Bargeman, E.D. Sprengers, C.A. Smolders, Characterization of hollow fiber hemodialysis membranes: pore size distribution and performance, *J. Membr. Sci.* 73 (1992) 143–152, [https://doi.org/10.1016/0376-7388\(92\)80124-3](https://doi.org/10.1016/0376-7388(92)80124-3).
- [25] M. Tagaya, S. Nagoshi, M. Matsuda, S. Takahashi, S. Okano, K. Hara, Hemodialysis membrane coated with a polymer having a hydrophilic blood-contacting layer can enhance diffusional performance, *Int. J. Artif. Organs* 40 (2017) 665–669, <https://doi.org/10.5301/ijao.5000631>.
- [26] C.M. Kee, A. Idris, Permeability performance of different molecular weight cellulose acetate hemodialysis membrane, *Sep. Purif. Technol.* 75 (2010) 102–113, <https://doi.org/10.1016/j.seppur.2010.08.013>.
- [27] Y. Seita, A. Mochizuki, M.N. Agawa, A. Takanashi, S. Yamashita, Polyether-
- segmented nylon hemodialysis membranes. I. Preparation and permeability characteristics of polyether-segmented nylon 610 hemodialysis membrane, *J. Appl. Polym. Sci.* 65 (1997) 1703–1711, [https://doi.org/10.1002/\(SICI\)1097-4628\(19970829\)65:9<1703::AID-POLB1097>3.0.CO;2-J](https://doi.org/10.1002/(SICI)1097-4628(19970829)65:9<1703::AID-POLB1097>3.0.CO;2-J).
- [28] A. Mochizuki, Y. Seita, F. Endo, T. Nishi, N. Saiga, S. Yamashita, Polyether-segmented nylon hemodialysis membranes. II. morphologies and permeability characteristics of polyether-segmented nylon 610 membrane prepared by the phase inversion method, *J. Appl. Polym. Sci.* 65 (1997) 1713–1721 <<http://doi.wiley.com/10.1002/%28SICI%291097-4628%2819970829%2965%3A9%3C1703%3A%3AID-APP6%3E3.0.CO%3B2-J>>.
- [29] K. Sakai, Determination of pore size and pore size distribution: 2. Dialysis membrane, *J. Membr. Sci.* 96 (1994) 91–130, [https://doi.org/10.1016/0376-7388\(94\)00126-X](https://doi.org/10.1016/0376-7388(94)00126-X).
- [30] P. Röder, B. Wu, Y. Liu, W. Han, Pancreatic regulation of glucose homeostasis, *Exp. Mol. Med.* 48 (2016), <https://doi.org/10.1038/emm.2016.6>.
- [31] G.L. Miller, Use of dinitrosalicylic acid reagent for determination of reducing sugar, *Anal. Chem.* 31 (1959) 426–428, <https://doi.org/10.1021/ac60147a030>.
- [32] P. Cañizares-Macías, L. Hernández-Garciadiego, H. Gómez-Ruiz, An automated flow injection analysis procedure for the determination of reducing sugars by DNSA method, *J. Food Sci.* 66 (2001) 407–411, <https://doi.org/10.1111/j.1365-2621.2001.tb16118.x>.
- [33] A. Gabelman, S.-T. Hwang, Hollow fiber membrane contactors, *J. Membr. Sci.* 159 (1999) 61–106, [https://doi.org/10.1016/S0376-7388\(99\)00040-X](https://doi.org/10.1016/S0376-7388(99)00040-X).
- [34] H. Estay, M. Ortiz, J. Romero, A novel process based on gas filled membrane absorption to recover cyanide in gold mining, *Hydrometallurgy* (2013) 134–135, <https://doi.org/10.1016/j.hydromet.2013.02.012>.
- [35] H. Estay, S. Bocquet, J. Romero, J. Sánchez, G.M. Rios, F. Valenzuela, Modeling and simulation of mass transfer in near-critical extraction using a hollow fiber membrane contactor, *Chem. Eng. Sci.* 62 (2007) 5794–5808, <https://doi.org/10.1016/j.ces.2007.05.037>.
- [36] R.B. Bird, W.E. Stewart, E.N. Lightfoot, *Transport Phenomena, Second*, John Wiley & Sons, 2002.
- [37] E.L. Cussler, *Diffusion: Mass Transfer in Fluid Systems*, 3rd ed., New York, 2009, pp. 237–331.
- [38] M.-C. Yang, E.L. Cussler, Designing hollow-fiber contactors, *AIChE J.* 32 (1986) 1910–1916, <https://doi.org/10.1002/aic.690321117>.
- [39] R. Gawroński, B. Wrzesińska, Kinetics of solvent extraction in hollow-fiber contactors, *J. Membr. Sci.* 168 (2000) 213–222, [https://doi.org/10.1016/S0376-7388\(99\)00317-8](https://doi.org/10.1016/S0376-7388(99)00317-8).
- [40] D. Green, R. Perry, *Perry's Chemical Engineers' Handbook*, 8th ed., McGraw-Hill, New York, 2008, <https://doi.org/10.1036/0071511245>.
- [41] Y. Cengel, *Heat and Mass Transfer: A Practical Approach*, 3rd ed., McGraw-Hill, India, 2007.
- [42] L. Normén, H.N. Laerke, B.B. Jensen, A.M. Langkilde, H. Anderson, Small-bowel absorption of D-tagatose and related effects on carbohydrate digestibility: an ileostomy study, *Am. J. Clin. Nutr.* 73 (2001) 105–110, <https://doi.org/10.1093/ajcn/73.1.105>.
- [43] K. Fine, C. Santanna, J. Porter, J. Fordtran, Effect of changing intestinal flowrate on a measurement of intestinal permeability, *Gastroenterology* 108 (1995) 983–989.
- [44] N.A. Blackburn, J.S. Redfern, H. Jarjis, A.M. Holgate, I. Hanning, J.H. Scarpello, I.T. Johnson, N.W. Read, The mechanism of action of guar gum in improving glucose tolerance in man, *Clin. Sci.* 66 (1984) 329–336, <https://doi.org/10.1042/cs0660329>.
- [45] C. Feng, B. Shi, G. Li, Y. Wu, Preparation and properties of microporous membrane from poly(vinylidene fluoride-co-tetrafluoroethylene) (F2.4) for membrane distillation, *J. Membr. Sci.* 237 (2004) 15–24, <https://doi.org/10.1016/j.memsci.2004.02.007>.
- [46] S. Simone, A. Figoli, A. Criscuoli, M.C. Carnevale, A. Rosselli, E. Drioli, Preparation of hollow fibre membranes from PVDF/PVP blends and their application in VMD, *J. Membr. Sci.* 364 (2010) 219–232, <https://doi.org/10.1016/j.memsci.2010.08.013>.
- [47] K. Schulze, Imaging and modelling of digestion in the stomach and the duodenum, *Neurogastroenterol. Motil.* 18 (2006) 172–183, <https://doi.org/10.1111/j.1365-2982.2006.00759.x>.
- [48] H. Helander, L. Fandriks, Surface area of the digestive tract - revisited, *Scand. J. Gastroenterol.* 49 (2014) 681–689, <https://doi.org/10.3109/00365521.2014.898326>.
- [49] R. Fisher, L. Malmud, P. Bandini, E. Rock, Gastric emptying of a physiologic mixed solid-liquid meal, *Clin. Nucl. Med.* 7 (1982) 215–221.
- [50] P. Hellstrom, P. Gryback, H. Jacobsson, The physiology of gastric emptying, *Best. Pr. Res. Clin. Anaesthesiol.* 20 (2006) 397–407.
- [51] M.J. Ferrua, R.P. Singh, Human gastric simulator, in: K. Verhoeckx, P. Cotter, I. López-Expósito, C. Kleiveland, T. Lea, A. Mackie, T. Requena, D. Swiatecka, H. Wichers (Eds.), *Impact Food Bioact. Heal. Vitr. Ex Vivo Model*. Springer, 2015, <https://doi.org/10.1007/978-3-319-16104-4>.